DEVELOPMENTAL BIOLOGY 177, 232–249 (1996)
ARTICLE NO. 0159

Targeted Disruption of *hoxc-4* Causes Esophageal

Anne M. Boulet and Mario R. Capecchi[1]
Department of Human Genetics, Howard Hughes Medical Institute, University of Utah School of Medicine, Salt Lake City, Utah 84112

Mice carrying a nonfunctional allele of *hoxc-4* have been generated by gene targeting. The phenotype of mice homozygous for this mutation is strikingly different from those reported in mice lacking the paralogous genes *hoxa-4*, *hoxb-4*, and *hoxd-4*. In contrast to the mutants of the paralogous family members, *hoxc-4* homozygotes do not manifest abnormalities in the cervical vertebrae, but instead show vertebral defects that extend from the second thoracic vertebra (t2) to t11. Therefore, defects do not correspond to the anterior limit of expression of *hoxc-4*, but rather begin within the region of strong *hoxc-4* expression in the prevertebral anlagen (i.e., pv7–14). While *hoxc-4* mutant homozygotes that reach adulthood are fertile and appear outwardly normal, most die before weaning age. The high lethality appears to result from partial or complete blockage of the lumen of the esophagus over a large portion of its length, as well as disorganization of the esophageal musculature. Although the *Drosophila* homolog of *hoxc-4*, *Deformed*, is autoregulated, mutation of the *hoxc-4* gene does not affect transcription of its paralogous family members. However, in *hoxc-4* mutant embryos, transcription of both the *hoxc-5* and *hoxc-6* genes is altered. Employment of cis/trans analysis showed that the *hoxc-4* mutation acts in cis to affect the pattern of *hoxc-5* expression. Therefore, this mutation is likely to cause a reduction of *hoxc-5* function as well as complete loss of *hoxc-4* function.

INTRODUCTION

Several studies have now established that genes of the *Hox* complex play key roles in embryonic development of the mouse. The 39 genes that comprise the *Hox* complex are arranged in four linkage groups, Hox A, B, C, and D. *Hox* genes have been divided into 13 paralogous groups based on sequence similarity and position within each cluster. The genes in each cluster are transcribed in the same direction such that each cluster has a 5′ to 3′ orientation. The anterior boundaries of expression in the nervous system and in the prevertebral column are colinear with the order of genes on the chromosome (Duboule and Dollé, 1989; Graham *et al.*, 1989). The 3′ *Hox* genes are expressed in anterior regions while the 5′-most genes are only expressed in the most posterior regions of the embryo and in the developing limbs.

Analysis of mice carrying mutations in *hoxa-1*, *hoxa-2*, and *hoxa-3* indicates that the 3′ genes are involved in the development of the hindbrain and neural crest derivatives (Chisaka and Capecchi, 1991; Lufkin *et al.*, 1991; Chisaka *et al.*, 1992; Carpenter *et al.*, 1993; Gendron-Maguire *et al.*, 1993; Mark *et al.*, 1993; Rijli *et al.*, 1993; Manley and Capecchi, 1995). *Hox* genes with rostral expression boundaries in the most posterior regions of the embryo function in the development of the caudal realm of the embryo and in the appendicular skeleton (Dollé *et al.*, 1993; Small and Potter, 1993; Davis and Capecchi, 1994; Satokata *et al.*, 1995). Genes from paralogous groups 3 through 13 are required for the proper formation of the axial skeleton. Thus, loss of function mutations for *hoxa-4*, *hoxa-5*, *hoxa-6*, *hoxa-10*, *hoxa-11*, *hoxb-4*, *hoxb-5*, *hoxb-6*, *hoxc-8*, *hoxc-9*, *hoxd-3*, *hoxd-4*, *hoxd-11*, and *hoxd-13* clearly demonstrate that the establishment of vertebral identity is dependent on the function of these genes (LeMouellic *et al.*, 1992; Condie and Capecchi, 1993; Dollé *et al.*, 1993; Jeannotte *et al.*, 1993; Ramirez-Solis *et al.*, 1993; Small and Potter, 1993; Davis and Capecchi, 1994; Kostic and Capecchi, 1994; Horan *et al.*, 1995a; Rancourt *et al.*, 1995; Satokata *et al.*, 1995; Suemori *et al.*, 1995). In addition, overexpression and/or misexpression of *hoxa-7*, *hoxb-7*, *hoxb-8*, *hoxc-6*, *hoxc-8*, and *hoxd-4* result in transformation of axial skeletal structure (Kessel *et al.*, 1990; Jegalian and DeRobertis, 1992; Lufkin *et al.*, 1992; McLain *et al.*, 1992; Pollock *et al.*, 1992, 1995).

[1] To whom correspondence should be addressed.

0012-1606/96 $18.00

Although axial defects can be expected in most cases, the specific malformations caused by mutations in *Hox* genes are difficult to predict. Some of this difficulty can be attributed to overlap of function between genes of the same paralogous group or even between genes of different paralogous groups (Condie and Capecchi, 1994; Davis *et al.*, 1995; Rancourt *et al.*, 1995; Davis and Capecchi, 1996). The direction of homeotic transformation of vertebrae seen in *Hox* mutants is also unpredictable. Both loss of function and gain of function mutations have shown anterior and posterior homeotic transformations. In fact, the two polarities of transformation can appear in the same mutant (Jeannotte *et al.*, 1993; Small and Potter, 1993). In *Drosophila*, anterior homeotic transformations occur in cases where the product of one gene negatively regulates transcription of a more anteriorly expressed gene (Hafen *et al.*, 1984; Struhl and White, 1985). When the regulating gene is mutated, the domain of expression of the more anterior gene is extended posteriorly. The structures within the new domain are transformed to a more anterior identity. Similarly, posterior transformations are caused by ectopic expression of more posteriorly expressed genes either because these proteins are phenotypically dominant or because expression of the more anterior genes is repressed (Gonzales-Reyes and Morata, 1990). There is no evidence thus far that the phenotypes observed in *Hox* gene mutants can be explained by analogous mechanisms.

It has been suggested that posterior prevalence explains the phenotype of mice mutant for a single *Hox* gene (Duboule, 1991). In this model, the identity of axial structures is determined by the action of the most posterior *Hox* gene expressed at a particular axial level. As a consequence, mutation of a single *Hox* gene would be expected to show a phenotype at the axial level at which it is the most posterior *Hox* gene expressed, i.e., at the anterior boundary of its expression pattern. However, this model has not correctly predicted mutant phenotypes in a number of cases. While mutations in some *Hox* genes affect structures derived from the most anterior portion of the expression domain (*hoxa-1*, *hoxa-2*, and *hoxa-3*, for example), other *Hox* gene knockouts have more far-reaching consequences. For example, *hoxb-4* mutants show defects in the sternum as well as the second and third cervical vertebrae, and *hoxa-5*$^{-/-}$ mice show a transformation of the first lumbar (L1) vertebra toward a thoracic identity (Ramirez-Solis *et al.*, 1993; Jeannotte *et al.*, 1993). Thus, the transformations observed in *Hox* gene mutants often occur in regions of the axial skeleton that express a number of more posterior *Hox* genes.

Another model proposes that it is the combination of *Hox* genes expressed that determines the identity of structures derived from cells of a particular region of the embryo (Kessel and Gruss, 1991). From a broad perspective, this model is undoubtedly correct since evidence clearly demonstrates that the formation of specific structures is dependent on the concerted action of two or more *Hox* genes. For example, in the absence of *hoxa-3* and *hoxd-3*, the atlas is not formed and in the absence of *hoxa-11* and *hoxd-11*, the radius and ulna are not formed (Condie and Capecchi, 1994; Davis *et al.*, 1995). However, specific combinatorial models based on overlapping *Hox* gene expression patterns do not accurately predict vertebral identity. Instead, it appears that the interactions between *Hox* genes that determine vertebral form are much more complex and must be functionally determined on a case by case basis through the analysis of individual as well as appropriate combinations of *Hox* gene mutations.

Phenotypes of *hoxa-4*, *hoxb-4*, and *hoxd-4* mutant mice have been described and all three show defects in development of the cervical vertebrae at the anterior limits of their respective expression domains (Ramirez-Solis *et al.*, 1993; Horan *et al.*, 1994, 1995a; Kostic and Capecchi, 1994). To address the role of *hoxc-4*, we generated mice that carry a loss of function mutation of this gene. In *hoxc-4* mutant mice, vertebral defects were seen posterior to the anterior limit of the *hoxc-4* expression domain and were detected over a long axial distance including most of the thoracic vertebrae. Although the rostral boundary of *hoxc-4* expression in the prevertebrae is at pv4, slightly more posterior than those of the paralogous genes, t2 was the most anterior position affected (i.e., pv9). In addition to vertebral defects, *hoxc-4* mutant mice showed severe defects in the physiological function of the esophagus. The lumen of the esophagus was partially or completely blocked over a large portion of its length and the esophageal musculature was disorganized. The latter phenotype is likely to account for the high mortality of *hoxc-4* mutant homozygotes.

MATERIALS AND METHODS

Targeted Mutagenesis of the hoxc-4 Locus

Phage clones containing the *hoxc-4* gene were isolated from a library prepared from CC1.2 ES cell line DNA using oligonucleotide probes derived from the published sequence of human *hox3E* (*hoxc-4*) (Simeone *et al.*, 1988). DNA sequencing confirmed the identity of the isolated gene. This sequence is nearly identical to the sequences published by Geada *et al.* (1992) and Goto *et al.* (1993). A replacement type targeting vector was constructed with the *pol2neo* cassette (Thomas and Capecchi, 1987; Deng *et al.*, 1993) inserted at the *Xho*I site between the third and the fourth codons of the *hoxc-4* homeobox. Homology 3′ (1.7 kb) and homology 5′ (9.2 kb) to the *neo* insertion site were included in the targeting vector, which was flanked by the TK1 and TK2 genes (Fig. 1A). The *hoxc-4* targeting vector was electroporated into AB1 cells (McMahon and Bradley, 1990). Thirteen targeted cell lines out of 96 isolated clones were obtained. Five cell lines were subjected to further analysis on Southern blots. No rearrangements within 8 kb on either side of the *hoxc-4* gene were detected, and each clone contained only one copy of the *pol2neo* cassette. Three cell lines were injected into blastocysts and independent germline chimeras were produced. Chimeras and germline progeny were crossed to C57Bl/6 females resulting in a hybrid 129SvEv-C57Bl/6 background.

Pups and newborns were genotyped by PCR analysis of tail or

skin DNAs. The genotype of embryos was determined by PCR analysis of yolk sac DNAs. PCR primers were derived from the *hoxc-4* intron (5′ primer, *hoxc-4*), the HPRT sequences at the 3′ end of the *pol2neo* cassette (5′ *neo* primer), and *hoxc-4* coding sequences 3′ of the homeobox (3′ primer). PCR products were separated on 5% acrylamide gels or 1.5% trevigels. The resulting products were 408 bp (wild-type band) and 308 bp (mutant band).

Production of Anti-hoxc-4 Antibodies

A 253-bp region from the first exon of the *hoxc-4* gene (encoding amino acids 34–117 of the *hoxc-4* protein) was fused in-frame to the GST coding sequence in the vector pGEX-KG. The 84-amino-acid region of *hoxc-4* fused to GST shows little homology to the paralogous genes *hoxa-4*, *hoxb-4*, and *hoxd-4*. Antibodies were generated by BAbCO (Richmond, CA) by injection of purified fusion protein into rabbits. Antibodies were depleted of anti-GST antibodies and affinity purified with *hoxc-4* fusion protein.

Whole-Mount Antibody Staining and in Situ Hybridization

Whole-mount immunohistochemistry was carried out on embryos genotyped by PCR analysis of yolk sac DNA using a protocol adapted from that described in Wall *et al.* (1992) and Rancourt *et al.* (1995). E12.5 embryos were dissected in PBS, fixed overnight in 4:1 methanol:DMSO, bleached in 4:1:1 methanol:DMSO:30% H_2O_2 for 6 hr, and stored at −20°C in methanol. Prior to staining, embryos were hemisected with a razor blade and rehydrated through a graded methanol series into PBST (0.5% Triton X-100 in PBS). After blocking in PBSTMD (2% instant skim milk, 1% DMSO in PBST), embryos were incubated in the anti-*hoxc-4* antibody, at a dilution of 1:50, in PBSTMD overnight at 4°C. Embryos were washed in PBST for 4 hr at room temperature. In some experiments, the embryos were blocked in PBSTMD prior to incubation with the secondary antibody. Incubation in donkey anti-rabbit HRP-conjugated secondary antibody (Jackson ImmunoResearch Laboratories), at a dilution of 1:500 in PBSTMD, was carried out overnight at 4°C. Washes were repeated, and, after a 1-hr incubation in 0.6 mg/ml DAB in PBST, H_2O_2 was added to a final concentration of 0.03%. Color reactions were stopped after 10 min by washing with PBST. The same protocol was used for staining with monoclonal antibody 2H3 (anti-155kD neurofilament protein; Dodd *et al.*, 1988) except that the primary antibody was diluted at 1:1, the goat anti-mouse HRP-conjugated secondary antibody was used at 1:200 (JIRL), and the color reactions were stopped after 1 min or less. In some experiments, chloronaphthol was used as the HRP substrate according to the protocol in Mark *et al.* (1993).

In situ hybridization on hemisected E12.5 embryos was carried out essentially as described (Carpenter *et al.*, 1993) except for the following modifications: probes were used at 0.5 μg/ml on hemisected E12.5 embryos; alkaline phosphatase-conjugated anti-digoxigenin antibody (Boehringer-Mannheim Biochemicals) was used at a dilution of 1:5000; levamisole was added to the alkaline phosphatase reaction buffer rather than to the blocking solution prior to antibody incubation; and the alkaline phosphatase substrate was BM purple (Boehringer-Mannheim Biochemicals). The *hoxa-4* probe was transcribed from a 0.7-kb *Xba*I–*Hin*dIII fragment from the 3′ untranslated region of the gene. For the *hoxb-4* probe, RNA transcripts were generated from a 450-bp *Nae*I–*Bam* fragment containing the last nine *hoxb-4* codons and 3′ untranslated sequences. The *hoxd-4* probe was transcribed from a 0.8-kb *Eco*RI fragment containing the entire first exon. The *hoxb-4* template and *hoxd-4* RNA probe were provided by N. Manley. The *hoxc-5* probe was derived from a 1-kb *Xba*–*Hin*dIII fragment consisting of 3′ untranslated sequence. A 5′ probe for *hoxc-5* was derived from a 0.8-kb *Eco*RV–*Bam*HI fragment containing the entire first exon of *hoxc-5*. The *hoxc-6* probe was transcribed from a PCR-generated 340-bp fragment extending from the end of the homeobox to a *Pst* site in the 3′ untranslated region. The *hoxc-5* and *hoxc-6* templates were constructed by D. Spyropoulos and O. Chisaka, respectively.

Histology and Skeleton Preparations

Newborn mice were asphyxiated with CO_2 and fixed at least 1 week in Bouin's fixative. Specimens were embedded in paraffin and sections of 12.5 μm were collected on slides. Sections were stained with hematoxylin and eosin.

Skeleton preparations of newborn and adult animals were carried out as described (Mansour *et al.*, 1993).

RESULTS

Generation of the hoxc-4 Mutant

The *hoxc-4* gene was cloned from a 129Sv mouse genomic DNA library. A replacement-type targeting vector was constructed by insertion of the *pol2neo* cassette into the *Xho*I site at nucleotide 10 of the homeobox (Fig. 1A; Deng *et al.*, 1993). The targeting vector was electroporated into AB1 cells, and 13 targeted cell lines were obtained. Three of these cell lines were injected into C57Bl/6 blastocysts to generate chimeric males capable of transmitting the mutant allele to their progeny. Southern blots were used to confirm the absence of any additional rearrangements in the region of the *hoxc-4* gene in the targeted cell lines and in heterozy-

FIG. 1. *Hoxc-4* gene targeting and analysis of genotypes. (A) Maps of the *hoxc-4* locus, the targeting vector used for mutagenesis, and the *hoxc-4 neo* allele. Black boxes denote the two exons of *hoxc-4*. The *pol2neo* gene and the *hoxc-4* gene are both transcribed from left to right. (B) Southern blot analysis of DNA from targeted ES cell line 1g-4 and tail DNA from two progeny of chimera 1150, N1 and N2. DNAs were digested with either *Eco*RV or *Xba*. Blots were probed with the 5′ probe, a 0.8-kb *Eco*RV–*Spe*I fragment, or the 3′ probe, a 3.3-kb *Eco*RI fragment, respectively. The endogenous *Eco*RV genomic fragment hybridizing with the 5′ probe is 15 kb. Insertion of the *pol2neo* cassette reduces the *Eco*RV fragment to 13 kb. The 3′ probe detects a shift in the size of the genomic *Xba*I fragment from 13 to 7.8 kb. (C) Genotype analysis of the progeny from a cross between two mice heterozygous for the *hoxc-4* mutation. An *Sst*I digest of tail DNA was probed with an internal probe. The endogenous *Sst*I fragment of 6.8 kb is shifted to 9.1 kb by the *pol2neo* insertion.

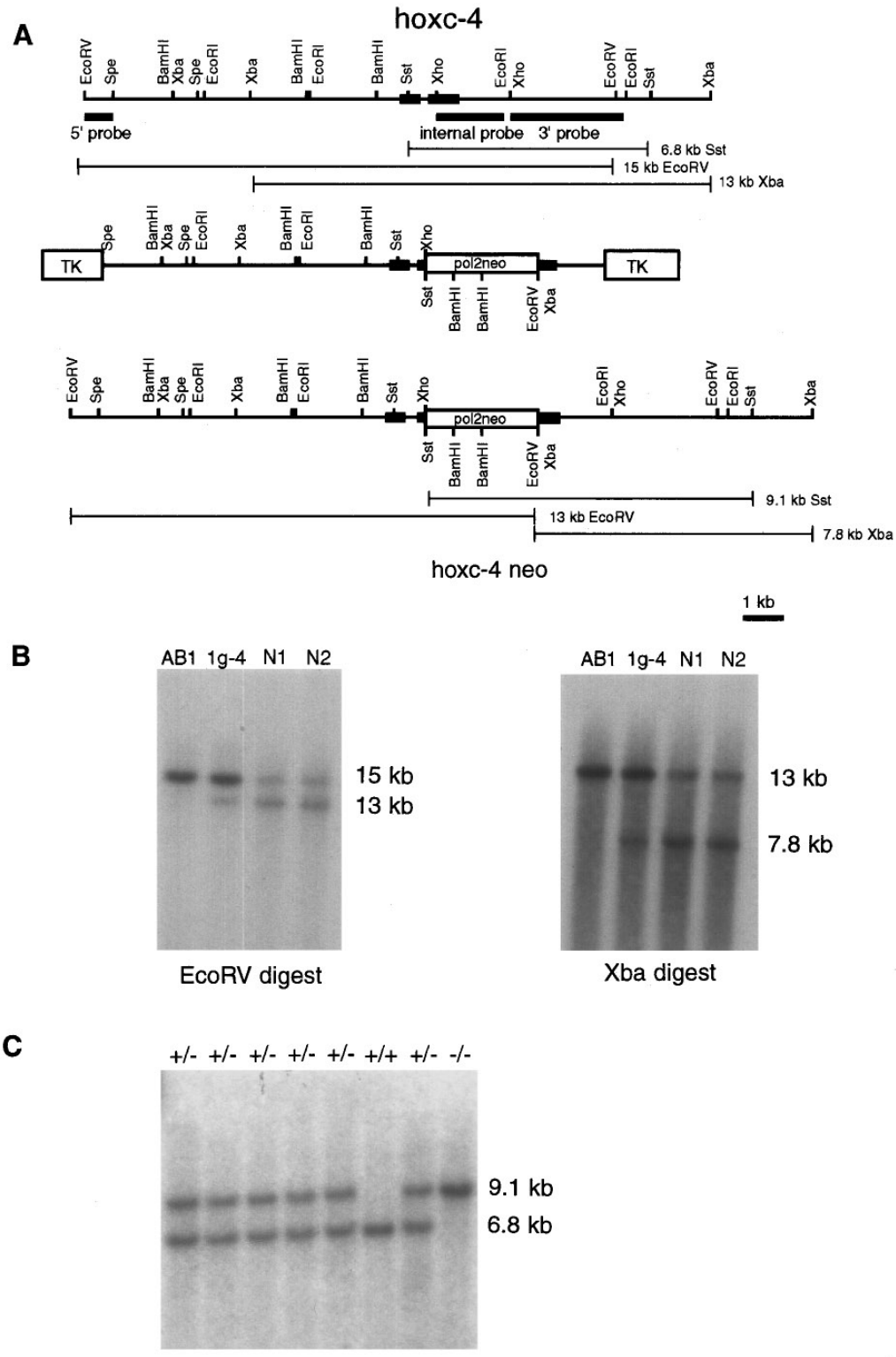

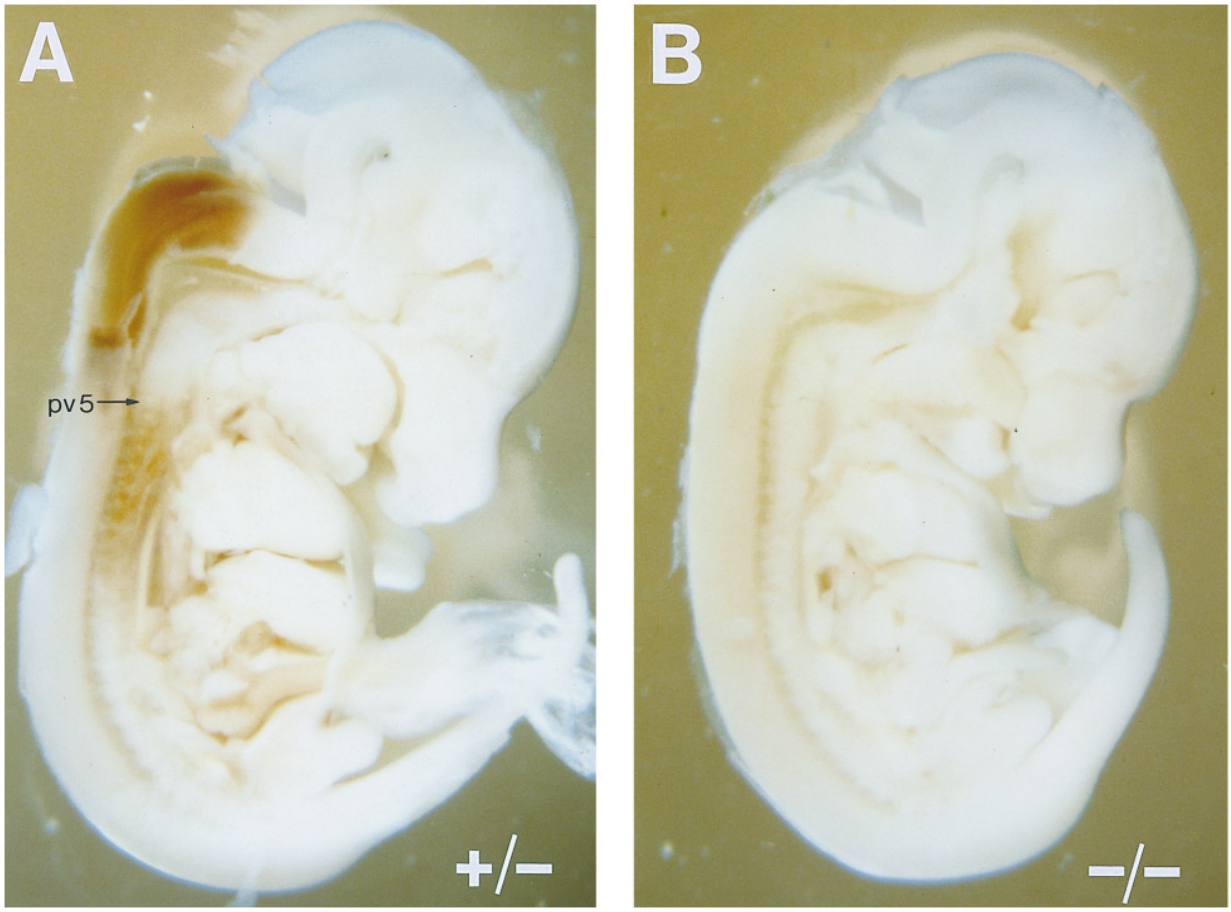

FIG. 2. Anti-*hoxc-4* antibody staining of embryos. (A) Hemisected *hoxc-4* heterozygous E12.5 embryo. In this experiment, *hoxc-4* protein was not detected anterior to prevertebra 5. (B) Hemisected E12.5 embryo homozygous for the *hoxc-4* mutation.

gous progeny (Fig. 1B). Hybridization of these blots with a *neo* probe ruled out the existence of additional random insertions of the targeting vector (data not shown). Heterozygous intercrosses were set up to examine the phenotype of mice homozygous for the *hoxc-4* mutation (Fig. 1C). Subsequent genotype analysis was accomplished by PCR assays.

A polyclonal antibody directed against the *hoxc-4* protein was used to confirm the absence of the *hoxc-4* gene product in homozygous mutant embryos. Homozygous *hoxc-4*$^{-}$ embryos at E12.5 (Fig. 2B) and E11.5 (data not shown) showed no detectable staining with the antibody while heterozygous littermates showed the expected *hoxc-4* pattern (Fig. 2A).

Viability and Fertility

Genotype analysis of progeny weaned from heterozygous *hoxc-4* mutant intercrosses demonstrated that homozygous *hoxc-4* mutant mice often died before weaning age (4 weeks). Of 166 intercross progeny, only 17 (10%) were homozygotes (Table 1). In contrast, when newborn mice from intercross litters were genotyped, the number of homozy-

FIG. 3. Skeletal defects in *hoxc-4* mutant newborn mice. (A, B) The lower cervical and upper thoracic region of a wild-type newborn mouse (A) and of a homozygous *hoxc-4* mutant (B). The open arrow in (B) marks the abnormally large dorsal process on the third thoracic vertebra of the mutant. (C, D) Rib cages of a wild-type mouse (C) and a *hoxc-4*$^{-/-}$ newborn (D). In the mutant (D), the eighth ribs are attached to the sternum (arrow), and a small fifth sternebra appears between ribs six and seven. (E, F) Dorsal views of vertebrae t8 through t12 in wild-type (E) and *hoxc-4* mutant (F) newborn skeletons stained with alizarin red. Arrows point to the transitional vertebrae; the ossified portion of the neural arch has a more rounded shape than more rostral vertebrae.

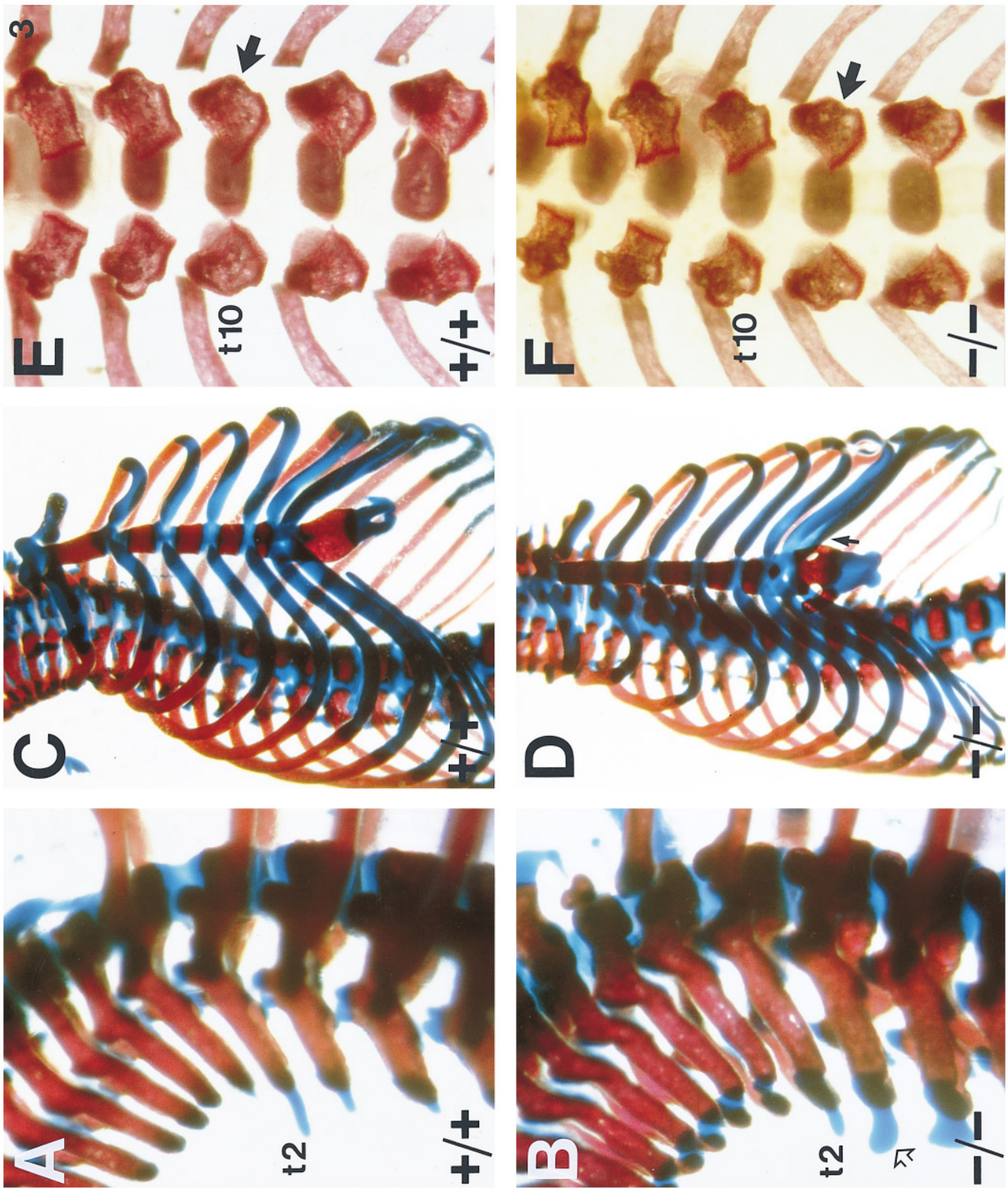

TABLE 1
Viability of *hoxc-4* Mutant Mice

	+/+	+/−	−/−	Total
+/− × +/−				
Newborns	20	39	17	76
Weaning age	54	95	17	166
+/− × −/−				
Newborns	—	16	17	33
Weaning age	—	39	21	60

gotes did not differ significantly from that expected. Thus, mice lacking the *hoxc-4* gene product survive embryogenesis, but often die before 4 weeks of age. Observation of newborn litters suggests that death occurs within the first day or two after birth. Animals destined to die appear to breathe and move normally, but at death have little or no milk in their stomachs.

The *hoxc-4* homozygotes that survived to weaning age tended to be smaller than their siblings, but otherwise appeared normal. Both male and female surviving homozygous *hoxc-4*$^{-}$ mice were fertile and no further lethality after weaning age was apparent.

Skeletal Phenotype

Examination of cleared skeleton preparations of *hoxc-4* homozygous mutant mice revealed a number of abnormalities in the thoracic region, from the 2nd to the 11th thoracic vertebra.

A large dorsal process, called the processus spinosus, is found on the second thoracic vertebra (t2) in normal mice. This process was absent or greatly reduced in size in all newborn and adult *hoxc-4*$^{-}$ homozygous skeletons examined (Table 2; Figs. 3A and 3B; Figs. 4A and 4B). In wild-type mice, the third thoracic vertebra has a smaller dorsal process than that found on t2. In 97% of homozygous mutant newborn animals examined, the dorsal process on t3 was significantly larger than that on t2 (Fig. 3B). In one *hoxc-4*$^{-/-}$ newborn, the dorsal processes on t2 and t3 were approximately the same size. In 3 of 35 heterozygous skeletons, the dorsal processes on t2 and t3 were approximately equal in size (data not shown; Table 2). In all 10 wild-type newborn skeletons examined, the t2 process was significantly larger than the t3 process. These results indicate that the second and the third thoracic vertebrae of homozygous *hoxc-4* mutants have been transformed toward the identities of the t1 and t2 vertebrae, respectively. The cervical and first thoracic vertebrae of all mutants showed normal morphology. In all 8 *hoxc-4*$^{-}$/*hoxc-4*$^{-}$ adult specimens examined, the length of the second and third pairs of ribs was reduced relative to ribs of wild-type animals (Figs. 4A and 4B). Heterozygous adult skeletons showed little or no evidence of t2 or t3 transformations (data not shown).

The first 7 of the 13 ribs normally found in wild-type mice are connected to the sternum while the last 6 ribs (on t8 through t13) are not attached (Fig. 3C). In *hoxc-4*$^{-}$ mutants, the eighth rib was often attached to the sternum on one or both sides (Fig. 3D; Table 2). The penetrance of this phenotype was 85% (extra vertebrosternal rib on one or both sides; Table 2). An eighth attached rib was found in 8% of the heterozygous mice examined, but in none of the wild-type littermates (Table 2). One of the three heterozygotes with an eighth vertebrosternal rib also had t2 and t3 processes of approximately equal size. All mutant homozygous skeletons showed 13 ribs and a normal number of lumbar vertebrae. *Hoxc-4*$^{-/-}$ mice occasionally exhibited a small fifth sternebra (Fig. 3D), but otherwise had normal sternum morphology.

The transitional thoracic vertebra is defined as the most anterior vertebra to show a lumbar rather than a thoracic articulation between the pre- and postzygapophyses (Pollock *et al.*, 1992, and references therein). In wild-type mice, the transitional vertebra is t10. In newborns, the ossified portion of the neural arch of t9 and more anterior vertebrae has a squared appearance (thoracic morphology) while that of t10, the transitional vertebra, and posterior vertebrae is more rounded (lumbar appearance). Because the articulations are difficult to examine in stained newborn skeleton preparations, the shape of the neural arch was used to score

TABLE 2
Skeletal Abnormalities of *hoxc-4* Mutant Newborns

	+/+	+/−	−/−
Dorsal process[a]			
t2 > t3	10 (100%)	32 (91%)	0
t2 = t3	0	3 (9%)	1 (3%)
t2 < t3	0		28 (97%)
Vertebrosternal ribs[b]			
7	10 (100%)	35 (92%)	5 (15%)
8 (one side)	0	2 (5%)	15 (44%)
8 (both sides)	0	1 (3%)	14 (41%)
Transitional vertebrae[c]			
t10	8 (80%)	16 (42%)	0
t10*	2 (20%)	19 (50%)	4 (12%)
t11	0	3 (8%)	29 (88%)

[a] The relative size of the dorsal process on the second thoracic vertebra and the third thoracic vertebra was scored in 10+/+, 35+/−, and 29−/− newborn skeletons.

[b] Ribs that were clearly joined to the sternum were scored as vertebrosternal. Ten+/+, 38+/−, and 34−/− newborn skeletons were examined.

[c] The most rostral vertebra in which the ossified portions of the neural arch have a rounded shape was scored as the transitional vertebra. If t10 showed an intermediate morphology, the transitional vertebra was designated t10*. The position of the transitional vertebra was determined in 10+/+, 38+/−, and 33−/− newborn mice.

the location of the transitional vertebra. The transitional vertebra corresponds to the first vertebra with a rounded neural arch (Figs. 3E and 3F). In *hoxc-4* homozygous mutants, the transitional vertebra is generally t11 (Table 2; Fig. 3F). In heterozygotes, t10 is often intermediate between a thoracic and lumbar morphology, and t11 is occasionally the transitional vertebra (Table 2). The transition between a thoracic and a lumbar type of articulation between zygapophyses can be seen after ossification of these structures has occurred in adult skeletal preparations stained with alizarin red. In wild-type animals, the postzygapophysis of t9 overlaps the prezygapophysis of t10 laterally (Fig. 5A). The lumbar type of articulation is seen between t10 and t11. The zygapophyses do not overlap as extensively, but appear to abut each other. In *hoxc-4*$^{-}$ homozygous adults, t10 showed the thoracic type of articulation with t9 and t11, and t11 was the transitional vertebra (Fig. 5B).

Differences in the expressivity of the t10 and t11 phenotypes can be seen when individual thoracic vertebrae are dissected from adult skeleton preparations. In four of eight mutant homozygous adults, t10 resembled t9 of wild-type littermates (Figs. 6A, 6B, 6D, and 6E) while t11 was strongly transformed toward t10 (Figs. 6C and 6F). In three mutant *hoxc-4* adults, t10 was transformed toward t9, and t11 was intermediate between a t10 and t11 morphology. The 8th mutant showed a transformation of t10 to t9, but a fairly normal t11 vertebra. In general, heterozygous adult skeletons show very weak transformations. The 10th thoracic vertebra of four of six adult heterozygotes showed some characteristics of t9, and weak transformations of t11 were apparent in 50% of heterozygotes (data not shown). Although the spinous process of t4 also appeared altered in shape relative to the wild-type in five of eight homozygous adults, the 5th through the 9th thoracic vertebral bodies do not possess features that can be used to unambiguously detect transformations of identity. However, it is clear that the *hoxc-4* mutation affects t2, t3, t8, t10, and t11.

Esophageal Defects in hoxc-4 Mutants

Since it appeared unlikely that skeletal defects in *hoxc-4*$^{-/-}$ animals could contribute to the high level of postnatal lethality observed, other tissues showing expression of *hoxc-4* during development were examined. No obvious defects in the nervous system were detected when E10.5 *hoxc-4* mutant embryos were stained with the neurofilament antibody 2H3 (data not shown). Since approximately 40% of the homozygotes do not carry a defect that results in postnatal lethality, a number of animals were examined.

Six newborn pups from a litter derived from a mating between a homozygous male and homozygous female were sectioned for H & E staining. Three of the pups died a short time before the remaining three newborns were sacrificed. Therefore, any phenotypes observed could be checked for correlation with the failure to survive. As described previously, *hoxc-4* is expressed in the esophagus (Geada *et al.*, 1992). In each of the three dead newborns, the esophagus was completely obstructed in some regions (Fig. 7B). None of the live newborns showed such a blockage (data not shown). The esophageal lumen and musculature of newborns not carrying the *hoxc-4* mutant allele that had died shortly after birth appeared histologically normal (data not shown). This result implies that the defects seen were not simply due to a failure to suckle or a delay between the time of death and fixation. The obstruction appeared to be caused by either proliferation of the epithelial cells lining the esophagus or a failure of the lumen to recanalize properly during development.

To investigate the possibility of a defect in recanalization of the lumen, homozygous mutant embryos were examined at E15.5, by which time the reopening process should be complete. In all eight *hoxc-4*$^{-/-}$ embryos sectioned, the lumen was opened along the entire extent of the esophagus. Therefore, recanalization appears to occur normally in *hoxc-4* mutant animals.

In the mouse, the external musculature of the cervical and most of the thoracic portion of the esophagus is composed of striated muscle cells. Smooth muscle cells appear in the lower thoracic region and eventually replace the striated muscle proximal to the stomach (Samarasinghe, 1972). In sagittal sections, the muscularis appears as two helical layers, wound in opposing directions. In cross-section, the two layers create a chevron pattern.

FIG. 4. Alterations in the second and third thoracic vertebrae and ribs of adult *hoxc-4* mutant mice. First (t1), second (t2), and third (t3) thoracic vertebrae and ribs of wild-type (A) and *hoxc-4* homozygous mutant mice (B). In the mutant, a large dorsal process is found on t3 rather than t2, and the length of the second pair of ribs is reduced compared to wild-type. Dorsal is down and anterior is facing out of the page.

FIG. 5. Transitional vertebrae in adult wild-type and *hoxc-4* mutant mice. (A) Lateral view of the lower thoracic region of a wild-type adult mouse. The transitional vertebra is t10. The articulation between t9 and t10 is of the thoracic type while the articulation between t10 and t11 resembles that of adjoining lumbar vertebrae. (B) Lateral view of a *hoxc-4* homozygous mutant adult. The articulations of t9 with t10 and of t10 with t11 are both of the thoracic type. The transitional vertebra is t11. White open arrows indicate the first articulation between zygapophyses having the lumbar morphology.

FIG. 6. Transformations of the 10th and 11th thoracic vertebrae. (A, B, C) Ninth, 10th, and 11th thoracic vertebrae (t9, t10, t11) of a wild-type adult mouse. (D, E, F) t9, t10, and t11 of a *hoxc-4* homozygous mutant mouse. p, prezygapophysis; po, postzygapophysis; tp, transverse process; sp, spinous process.

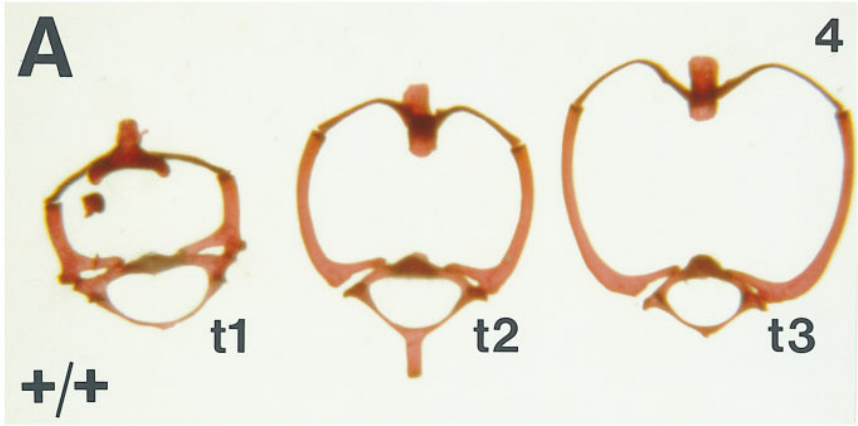
A
4
t1
t2
t3
+/+

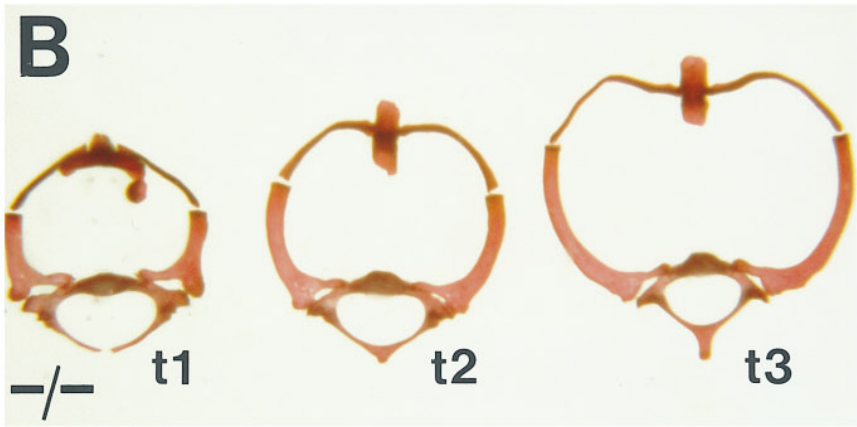
B
t1
t2
t3
–/–

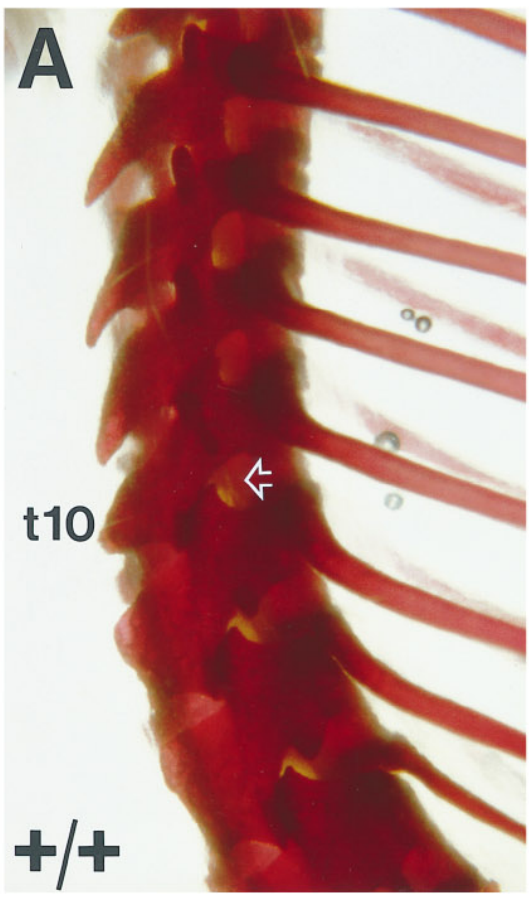
A
t10
+/+


B
5
t10
–/–

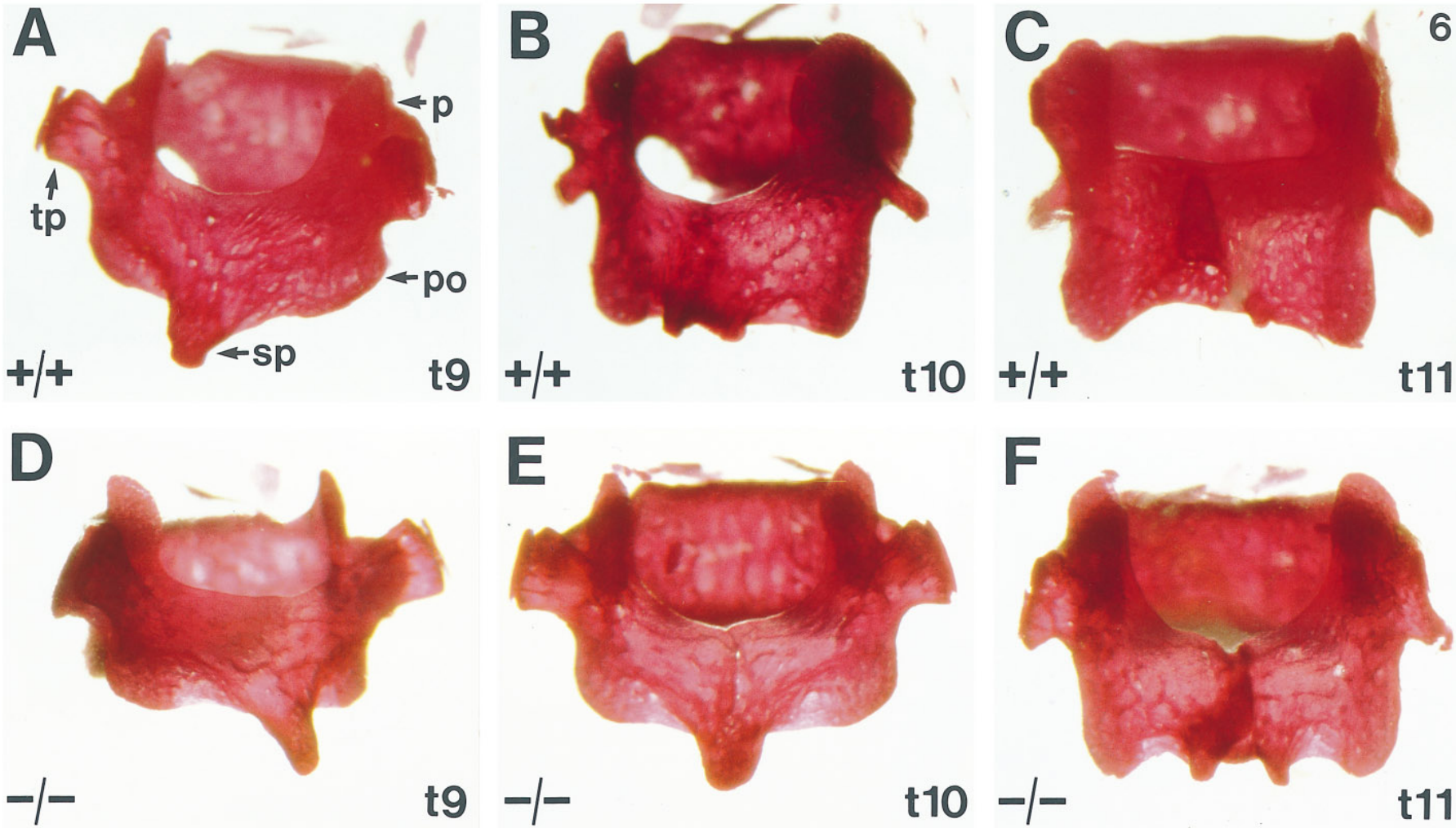
A
p
tp
po
sp
+/+
t9
B
+/+
t10
C
6
+/+
t11
D
−/−
t9
E
−/−
t10
F
−/−
t11

The muscle layers of the esophagus in the dead newborns appeared particularly disorganized over an extensive region (Fig. 7C). The live newborns showed some muscle disorganization, but this was not as severe as in the dead pups (data not shown). In contrast, other tissues in which *hoxc-4* is expressed in the embryo, such as the lungs and kidneys, did not show any morphological abnormalities.

Expression of Paralogous Genes

The *hoxc-4* gene belongs to the *Dfd*-related family of paralogs. The *Drosophila Deformed* gene is autoregulated: Dfd protein is required for transcription of the *Dfd* gene after initial activation (Kuziora and McGinnis, 1988). Therefore, it was of interest to determine whether the *hoxc-4* protein is required for its own transcription and the transcription of paralogous family members *hoxa-4, hoxb-4,* or *hoxd-4.*

Whole-mount *in situ* hybridization was used to examine RNA expression patterns in *hoxc-4* mutant animals at E12.5. These studies showed that *hoxc-4* protein is not required for its own expression nor did they uncover any changes in *hoxa-4, hoxb-4,* or *hoxd-4* expression at the embryonic stage examined (data not shown).

Effect of the hoxc-4 Mutation on hoxc-5 and hoxc-6 Expression

Transcription of the *hoxc-5* and *hoxc-6* genes was also examined in *hoxc-4* homozygous mutant embryos. In contrast to the results obtained with the paralogous genes, the pattern of *hoxc-5* expression was dramatically altered in homozygous *hoxc-4*$^{-}$ embryos at E10.5 (data not shown) and E12.5. Whereas wild-type embryos show an anterior limit of *hoxc-5* expression in the prevertebral column at pv5 or pv6 and high levels in pv7–15/16 (Gaunt *et al.,* 1990; Fig. 8A), the amount of *hoxc-5* RNA in *hoxc-4* mutant embryos is greatly reduced in the domain of strongest expression (Fig. 8C). In addition, *hoxc-5* is normally expressed in a region surrounding the forelimb (Fig. 8B). Staining with the *hoxc-5* probe is barely detectable in the corresponding region of *hoxc-4* homozygotes (Fig. 8D). Expression in the spinal cord of *hoxc-4*$^{-/-}$ embryos also shows a more posterior rostral boundary than seen in *hoxc-4* heterozygotes (Figs. 8A–8D). The pattern of *hoxc-6* transcription is also clearly affected by the *hoxc-4* mutation, albeit less severely than *hoxc-5.* The rostral boundary of *hoxc-6* expression in the prevertebral column is at pv7 or pv8 in heterozygotes, but at pv9 or pv10 in the *hoxc-4*$^{-/-}$ embryos (Figs. 8E and 8G). As seen for *hoxc-5,* the spinal cord expression domain of *hoxc-6* is also shifted posteriorly (Figs. 8E–8H).

To determine whether the alteration in *hoxc-5* expression was due to the absence of *hoxc-4* protein in the *hoxc-4* mutant homozygote, or due to a cis effect of the *hoxc-4* mutation on *hoxc-5* expression, we tested the ability of the *hoxc-4* protein to restore the wild-type pattern of *hoxc-5* expression in trans. This was accomplished by creating trans-heterozygous embryos in which one chromosome carries the *hoxc-4* mutation and the other chromosome carries a *hoxc-5* mutation (Fig. 9). Expression of the *hoxc-4* gene is not measurably affected by the *hoxc-5* mutation (data not shown). When *hoxc-5* homozygous embryos are hybridized with a probe containing sequences from the first exon of the *hoxc-5* gene (i.e., a probe 5′ of the *neo* insertion in the *hoxc-5* gene), an aberrant pattern of expression is observed (Figs. 10A and 10B). This pattern is readily distinguishable from that seen in wild-type embryos: the rostral boundaries of expression in the spinal cord and the prevertebral column are shifted and little or no expression is detected in the region surrounding the forelimbs. In *hoxc-5* heterozygotes, the *hoxc-5,* 5′ probe shows a pattern that is a combination of the wild-type and mutant patterns (Figs. 10C and 10D). If the *hoxc-4* protein is required in trans for *hoxc-5* transcription, the expression seen in the *hoxc-4*/*hoxc-5* trans-heterozygous embryos should also be the sum of the wild-type and mutant patterns. In contrast, if the *hoxc-4* mutation affects the transcription of *hoxc-5* in cis, the *hoxc-4* protein will not restore proper *hoxc-5* expression and trans-heterozygotes will display the *hoxc-5* mutant pattern plus the *hoxc-4* mutant pattern (Figs. 8C and 8D, Fig. 9). *Hoxc-4*/*hoxc-5* trans-heterozygous embryos clearly show a pattern that is the sum of the two mutant patterns (Figs. 10E and 10F), indicating that the *hoxc-4* mutation affects *hoxc-5* transcription in cis.

DISCUSSION

The skeletal phenotype caused by the mutation in *hoxc-4* was unexpected, especially in light of the results obtained with the paralogous genes *hoxa-4, hoxb-4,* and *hoxd-4.* The rostral expression boundaries of all four genes are located in the paraxial mesoderm destined to form cervical vertebrae, pv1 for *hoxb-4* and *hoxd-4,* pv2 for *hoxa-4,* and pv4 for *hoxc-4* (Gaunt *et al.,* 1989; Geada *et al.,* 1992). Mice homozygous for mutations in *hoxa-4, hoxb-4,* and *hoxd-4* show anterior homeotic transformations in the cervical vertebrae corresponding to their rostral expression boundaries (Ramirez-Solis *et al.,* 1993; Kostic and Capecchi, 1994; Horan *et al.,* 1994, 1995a). In contrast, the most rostral vertebral phenotype in *hoxc-4* mutant homozygotes is the anterior transformation of the second thoracic vertebra (pv9). Although anterior transformations of the fourth and fifth cervical vertebrae or posterior transformations of c3 or c4 would be difficult to discern, transformations of the sixth and seventh cervical vertebrae are easily scored. Therefore, the most anterior aspects of the vertebral column phenotype of *hoxc-4* homozygotes map to a region within the *hoxc-4* domain where expression is at a maximal level at E12.5, rather than the most anterior prevertebral location at which *hoxc-4* RNA and protein are detectable. The posterior boundary of *hoxc-4* function lies within the region in which *hoxc-4* expression is gradually decreasing to an undetectable

level in the prevertebral column (Geada *et al.*, 1992; Fig. 2A). It is unlikely that t2, t3, t8, t10, and t11 would be transformed to a more anterior identity without concomitant transformation of the intervening vertebrae. Thus, the region affected by the *hoxc-4* mutation is much more extensive than normally seen in mice with single *Hox* gene mutations.

The skeletal defects seen in *hoxc-4* mutant homozygotes are more akin to those seen when more posterior or 5′ *Hox* genes are inactivated. In particular, the appearance of an eighth vertebrosternal rib has been reported for *hoxc-8* mutant mice and in transgenic mice overexpressing either the *hoxc-8* or the *hoxc-6* gene products (Jegalian and DeRobertis, 1992; Pollock *et al.*, 1992; LeMouellic *et al.*, 1992). Transformations involving the transitional vertebra were also reported in transgenic mice overexpressing *hoxc-8.* An alteration of the position of the transitional vertebra has not been reported in other *Hox* gene mutant mice, but may not have been examined in all cases.

The extent of vertebral transformations observed in *hoxc-4* mutant mice may result in part from the effect of the *hoxc-4* mutation on *hoxc-5* and *hoxc-6* expression in the prevertebral column. Normally *hoxc-5* is expressed at high levels from pv7 to pv15/16 and at lower levels in pv5 and pv6 and from pv15 to the posterior end (Gaunt *et al.*, 1990). The expression in pv5 through pv15 is greatly reduced in *hoxc-4* mutant homozygotes. In addition, the rostral boundary of *hoxc-6* expression in the prevertebral column appears to be shifted posteriorly by two prevertebrae in *hoxc-4* mutant homozygotes. The regulation and function of these three genes appear to be closely intertwined. First, similarities in transcript distribution within the spinal cord and esophagus suggest that they may share common cis regulatory elements (Geada *et al.*, 1992). Second, in human cells transcripts have been found from these genes that are initiated from a common promoter (Simeone *et al.*, 1988). Finally, mutant homozygotes of these three genes show overlapping phenotypes (*hoxc-5,* A. Boulet, unpublished results; *hoxc-6,* D. Spyropoulos, unpublished results). However, the penetrance and expressivity of the skeletal defects are lower in *hoxc-5* and *hoxc-6* mutant homozygotes and both mutants are fully viable.

We have shown that the *hoxc-4* mutation affects transcription of the *hoxc-5* gene in cis. As mentioned above, *hoxc-4* and *hoxc-5,* the two most 3′ genes of the *HoxC* linkage group, show very similar patterns of gene expression (Gaunt *et al.*, 1990; Geada *et al.*, 1992, and herein). Therefore, the existence of shared regulatory elements would not be completely unexpected. The effect of the *hoxc-4* mutation on *hoxc-5* expression suggests that an enhancer located 3′ of *hoxc-4* or within the *hoxc-4* gene may be responsible for some aspects of *hoxc-5* expression. The *neo* insertion into *hoxc-4* may either directly disrupt this enhancer or interfere with its activity through enhancer competition. Interestingly, the *neo* insertion in *hoxc-4* is located more than 20 kb 3′ of the *hoxc-5* promoter. In a number of cases in which the *neo* gene insertion is much closer to adjacent *Hox* genes, we have not detected changes in the expression patterns of these genes. For example, a *neo* insertion into *hoxa-4* and *hoxa-6* does not influence the expression of the adjacent *Hox* genes (Kostic and Capecchi, 1994) and insertions in *hoxb-5* and *hoxb-6* do not affect transcription of *hoxb-6* and *hoxb-5,* respectively (Rancourt *et al.*, 1995).

Saegusa and colleagues (1996) have recently reported the phenotype of a *hoxc-4* mutant which differs from that described in this report in several respects. The *hoxc-4* allele of Saegusa *et al.* (1996) consists of a 0.6-kb deletion encompassing most of the homeobox and insertion of a *neo* gene driven by tandem promoters of SV40 and HSVtk. This mutation causes anterior transformations of t3 and t8, but at only half the penetrance seen for our allele. In addition, the Saegusa *et al.* allele does not cause any apparent reduction in viability. The dissimilarities between the phenotypes could be attributed to the use of different background strains of mice or to a difference in the effect of each mutation on the adjacent *hoxc-5* gene. Transcription of the *hoxc-5* gene was not examined by Saegusa *et al.* (1996). Disparate phenotypes for mutant Myf-6/MRF4 alleles appear to be due to the degree to which each mutation affects transcription of the neighboring Myf-5 gene (Braun and Arnold, 1995; Patapoutian *et al.*, 1995; Zhang *et al.*, 1995; Floß *et al.*, 1996). Differences in strain background have been shown to influence severity of the mutant phenotype in the case of *hoxb-4* (Ramirez-Solis *et al.*, 1993) and may be responsible for the observed difference between two alleles of *hoxa-4* (Kostic and Capecchi, 1994; Horan *et al.*, 1994).

As shown for *hoxc-4,* the effects of mutations in *Hox* genes on the formation of the vertebral column can often be interpreted in terms of changes in the shape of one or more vertebrae to resemble an adjacent anterior or posterior vertebra. These observations suggest that *Hox* genes are responsible for modifying a common vertebral module and thereby provide each vertebra with an identity. This could be accomplished, in part, by controlling, positively or negatively, the localized growth or recruitment of prechondrogenic precursor cells needed to form the vertebral modifications. Consistent with the above hypothesis, the expression patterns of *Hox* genes in the prevertebrae of the chick and mouse maintain register with the type of vertebrae rather than the position of the vertebrae along the vertebral column (Burke *et al.*, 1995). Also, combining mutations of the *hox-4* paralogous family (*hoxa-4, hoxb-4,* and *hoxd-4*) results in multiple cervical vertebrae acquiring characteristics associated with the first cervical vertebra (Horan *et al.*, 1995b). One interpretation of the latter result is that C1 may represent a ground state for cervical vertebrae and that the role of *hox-4* paralogous genes is to modify this basic module and thereby provide individuality to each cervical vertebra.

However, the role of *Hox* genes in mediating the formation of the vertebral column may be much more extensive than is apparent from the analysis of single *Hox* gene muta-

tions or of the *hox 4* paralogous genes. Probably all 39 *Hox* genes, in multiple combinations, are involved in forming the vertebral column. Individual *Hox* gene mutations may uncover only a small subset of their functions in specifying the vertebral column. A case in point is that *hoxa-3*$^{-/-}$ mice show no apparent vertebral defects, whereas *hoxd-3*$^{-/-}$ mice show defects in the formation of the first and second cervical vertebrae (Chisaka and Capecchi, 1991; Condie and Capecchi, 1993). However, combining these two mutations results in mice with the entire first cervical vertebra deleted (Condie and Capecchi, 1994). Ironically, this is the same vertebra that combinations of mutations in *hox-4* paralogous genes suggested might represent the cervical vertebral ground state. The results of *hoxa-3*, *hoxd-3* double mutants show that specific combinations of *Hox* mutations can abrogate the formation of an entire vertebra and brings into question the identity of the *Hox* ground state with respect to formation of the vertebral column. Resolution to this question will require combining multiple *Hox* gene mutations. It may not be practical to accomplish this aim by breeding together multiple single *Hox* gene mutations. Instead, more sweeping lesions that inactivate multiple *Hox* genes in a single step may be needed.

Three lines of evidence suggested that an autoregulatory loop involving genes with a *Dfd*-related homeobox has been conserved between *Drosophila* and mouse. The *Dfd* autoregulatory element appears to respond to transcriptional activators present in specific regions of the mouse embryo (Awgulewitsch and Jacobs, 1992); the human *hoxd-4* protein can function in *Drosophila* in a manner similar to the *Dfd* protein (McGinnis *et al.*, 1990); and a regulatory element of the human *hoxd-4* gene directs maxillary expression in late-stage *Drosophila* embryos (Malicki *et al.*, 1992). Therefore, it is surprising that the *hoxc-4* protein is not required for its own transcription or for transcription of paralogous genes. Consistent with this finding, the *hoxa-4* mutation does not influence transcription of *hoxc-4* (A. Boulet, unpublished), nor does the *hoxb-4* mutation alter *hoxa-4* or *hoxd-4* expression (Ramirez-Solis *et al.*, 1993). However, if the hypothetical autoregulatory function is redundant, transcriptional effects may only be seen in double, triple, or quadruple mutant embryos.

Defects in internal organs have been reported in *Hox* gene knockout mice and in mice overexpressing *Hox* gene family members. For example, *hoxa-3* mutant mice are athymic and aparathyroid and have reduced thyroid and submaxil-

FIG. 7. Defects in the esophagus of *hoxc-4* mutant newborns. (A) Transverse section of the esophagus from the upper thoracic region of a *hoxc-4*$^{+/-}$ newborn animal. (B, C) Transverse sections from the upper thoracic region of two *hoxc-4* homozygous mutant newborns that died shortly after birth. The section in (B) shows blockage of the lumen (open white arrow). Arrow in (C) marks disorganized area of muscle. e, stratified squamous epithelium; lu, lumen; s, submucosa; m, muscle layers.

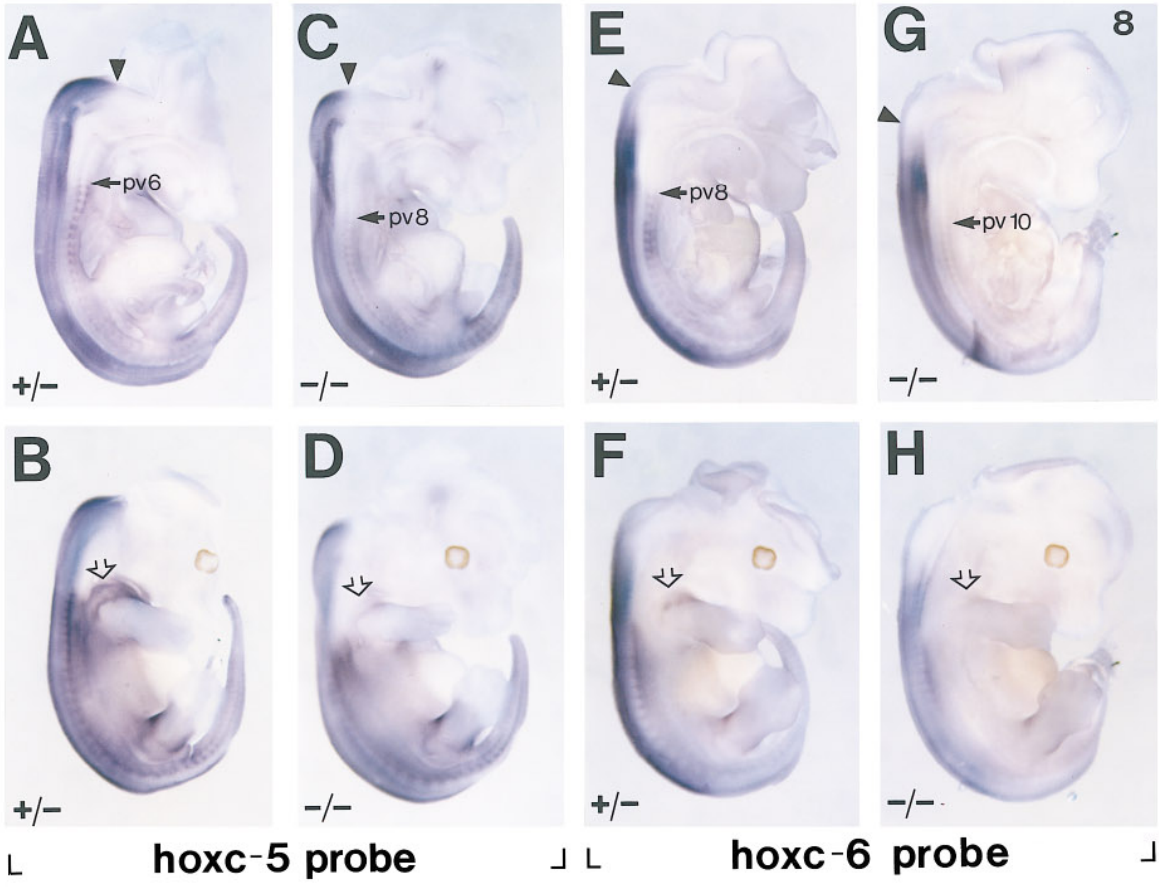
A
pv6
+/−
C
pv8
−/−
E
pv8
+/−
G
8
pv 10
−/−
B
+/−
D
−/−
F
+/−
H
−/−
hoxc-5 probe
hoxc-6 probe

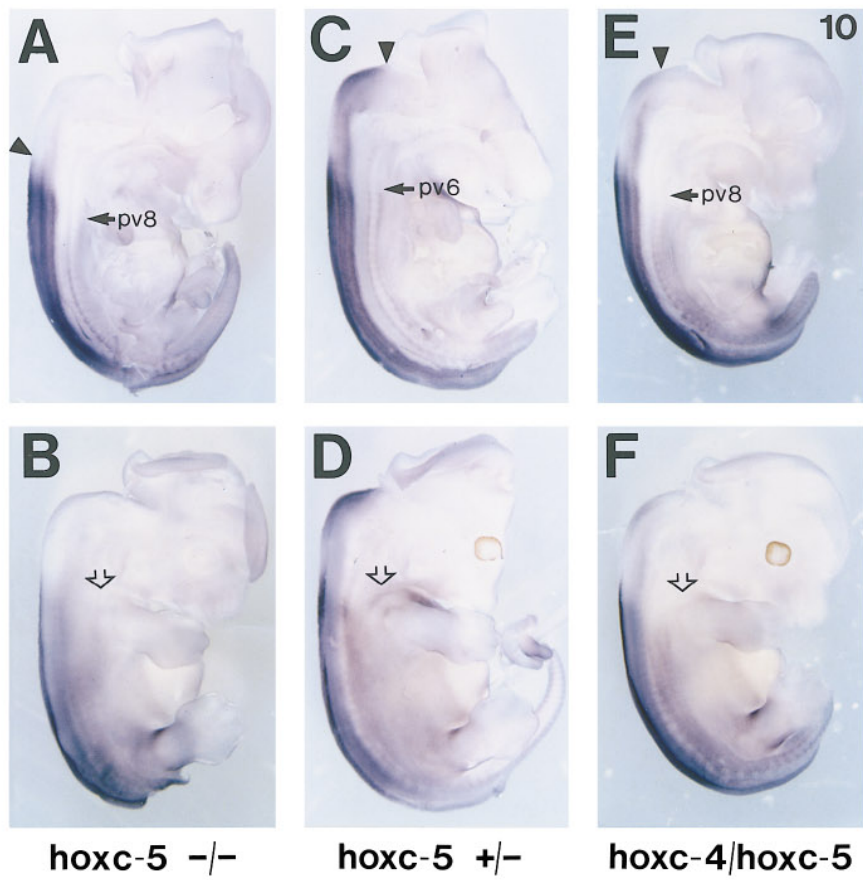
A
pv8
C
pv6
E
10
pv8
B
D
F
hoxc-5 −/−
hoxc-5 +/−
hoxc-4/hoxc-5

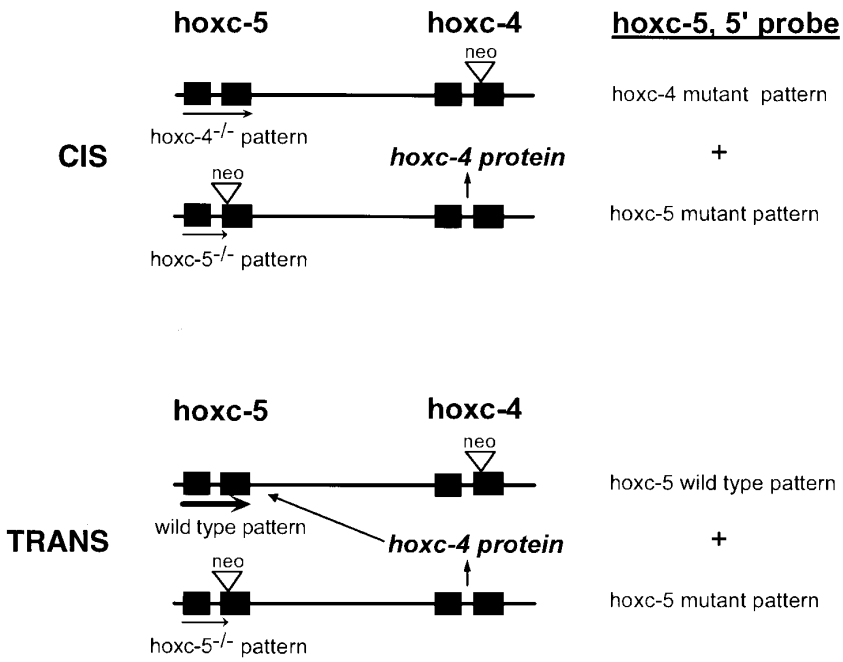

FIG. 9. Predicted outcomes for cis/trans test of *hoxc-4 neo* insertion effect on *hoxc-5* expression. The pairs of black lines represent the two homologous chromosomes in a trans-heterozygous *hoxc-4*/*hoxc-5* embryo. ''CIS'' shows the result expected if the *hoxc-4 neo* insertion exerts an effect on the *hoxc-5* gene on the same chromosome. ''TRANS'' shows the outcome expected if the *hoxc-4* protein is required to generate the wild-type *hoxc-5* expression pattern. *Hoxc-4* and *hoxc-5* exons are shown as black rectangles. Triangles represent the *neo* insertions in the mutant chromosomes. Thinner and shorter arrows beneath the *hoxc-5* gene represent aberrant patterns of *hoxc-5* transcription as detected by the *hoxc-5*, 5′ probe in *hoxc-4*$^{-/-}$ and *hoxc-5*$^{-/-}$ embryos, respectively. The thicker arrow under the *hoxc-5* gene designates a wild-type expression pattern.

lary tissue (Chisaka and Capecchi, 1991; Manley and Capecchi, 1995). They also show defects in the formation of the heart and arteries (Chisaka and Capecchi, 1991). *Hoxc-8* overexpression results in gastrointestinal tissue malformations and *hoxa-4* overexpression produces a megacolon phenotype (Wolgemuth *et al.*, 1989; Pollock *et al.*, 1992). On the other hand, most sites of *Hox* gene expression during organogenesis do not correlate with a phenotype in mice mutant for a given *Hox* gene. This may again be due to redundancy of function among the *Hox* complex members. For example, *hoxa-11* or *hoxd-11* mutant homozygotes do not show defects in the formation of the kidneys (Small and Potter, 1993; Hsieh-Li *et al.*, 1995; Davis and Capecchi, 1994). However, *hoxa-11* and *hoxd-11* double mutant homozygotes have severe kidney aplasia (Davis *et al.*, 1995). *Hoxc-4* mutant homozygotes show clear defects in the development of the esophageal lumen and musculature.

The esophageal cavity is formed by recanalization of the lumen from about E13 to E15 in the mouse. The presence of an open esophageal cavity in *hoxc-4* mutants at E15.5 strongly suggests that recanalization occurs normally and suggests that the observed blockage in *hoxc-4*$^{-/-}$ mice may

FIG. 8. Expression of the *hoxc-5* and *hoxc-6* genes in *hoxc-4* mutant embryos. (A–D) Hemisected E12.5 embryos hybridized with the *hoxc-5* probe. (A) *hoxc-4*$^{+/-}$, (B) *hoxc-4*$^{+/-}$ embryo surface, (C) *hoxc-4*$^{-/-}$, (D) *hoxc-4*$^{-/-}$ embryo surface. (E–H) Patterns of *hoxc-6* expression at E12.5. (E) *hoxc-4*$^{+/-}$, (F) *hoxc-4*$^{+/-}$ surface, (G) *hoxc-4*$^{-/-}$, (H) *hoxc-4*$^{-/-}$ surface. Arrowheads mark the approximate rostral boundary of *hoxc-5* or *hoxc-6* expression in the developing spinal cord. Open arrows in (B, D, F, H) point to the region of gene expression surrounding the forelimb described in the text.

FIG. 10. *Hoxc-5* expression in *hoxc-5* mutant and *hoxc-4*/*hoxc-5* trans-heterozygous embryos. Hemisected E12.5 embryos hybridized with the *hoxc-5*, 5′ probe. (A) *hoxc-5*$^{-/-}$, (B) *hoxc-5*$^{-/-}$ embryo surface, (C) *hoxc-5*$^{+/-}$, (D) *hoxc-5*$^{+/-}$ surface, (E) *hoxc-4*/*hoxc-5* trans-heterozygote, (F) *hoxc-4*/*hoxc-5* trans-heterozygote surface. Arrowheads mark the approximate rostral boundaries of *hoxc-5* expression in the spinal cord. Open arrows in (B, D, F) point to the region adjacent to the forelimb where *hoxc-5* expression is detected in wild-type embryos.

be due to overproliferation of the esophageal epithelial lining. Such a role would implicate *hoxc-4* in limiting rather than enhancing cell proliferation. The possibility of a defect in esophageal innervation should also be considered. If an esophageal defect is the sole contributor to the morbidity suffered by *hoxc-4*$^{-/-}$ mice, then the penetrance of this defect can be estimated to be 50 to 70%. A reduction of *hoxc-5* expression in the esophagus of *hoxc-4* mutants may contribute to the above phenotype; however, *hoxc-5* mutant homozygotes are fully viable and do not exhibit an esophageal defect.

In summary, we have demonstrated that mice homozygous for a targeted disruption of *hoxc-4* show apparent homeosis of vertebrae extending from t2 to t11. Unexpectedly, the point of initiation of these transformations does not correspond to the anterior limit of *hoxc-4* expression in the prevertebrae, but instead encompasses the entire region of high *hoxc-4* expression. The *hoxc-4* mutation affects the expression of *hoxc-5* and *hoxc-6* but not paralogous family members. Finally, our observations strongly suggest that *hoxc-4* mutant lethality results from esophageal dysfunction.

ACKNOWLEDGMENTS

We thank M. Allen, S. Barnett, C. Lenz, E. Nakashima, G. Peterson, and M. Wagstaff for excellent technical assistance. We are grateful to Paul Sharpe for providing *hoxc-5* cDNA sequence. L. Oswald helped with the preparation of the manuscript. The monoclonal antibody 2H3 was obtained from the Developmental Studies Hybridoma Bank maintained by the Department of Pharmacology and Molecular Sciences, Johns Hopkins University School of Medicine, Baltimore, Maryland, and the Department of Biological Sciences, University of Iowa, Iowa City, Iowa, under Contract N01-HD-6-2915 from the NICHD.

REFERENCES

Awgulewitsch, A., and Jacobs, K. (1992). Deformed autoregulatory element from *Drosophila* functions in a conserved manner in transgenic mice. *Nature* 358, 341–344.

Braun, T., and Arnold, H.-H. (1995). Inactivation of *Myf-6* and *Myf-5* genes in mice leads to alterations in skeletal muscle development. *EMBO J.* 14, 1176–1186.

Burke, A. C., Nelson, C. E., Morgan, B. A., and Tabin, C. (1995). *Hox* genes and the evolution of vertebrate axial morphology. *Development* 121, 333–346.

Carpenter, E. M., Goddard, J. M., Chisaka, O., Manley, N. R., and Capecchi, M. R. (1993). Loss of *Hox-A1* (*Hox-1.6*) function results in the reorganization of the murine hindbrain. *Development* 118, 1063–1075.

Chisaka, O., and Capecchi, M. R. (1991). Regionally restricted developmental defects resulting from targeted disruption of the mouse homeobox gene *hox-1.5*. *Nature* 350, 473–479.

Chisaka, O., Musci, T. S., and Capecchi, M. R. (1992). Developmental defects of the ear, cranial nerves and hindbrain resulting from targeted disruption of the mouse homeobox gene *Hox-1.6*. *Nature* 355, 516–520.

Condie, B. G., and Capecchi, M. R. (1993). Mice homozygous for a targeted disruption of *Hoxd-3* (*Hox-4.1*) exhibit anterior transformations of the first and second cervical vertebrae, the atlas and the axis. *Development* 119, 579–595.

Condie, B. G., and Capecchi, M. R. (1994). Mice with targeted disruptions in the paralogous genes *hoxa-3* and *hoxd-3* reveal synergistic interactions. *Nature* 370, 304–307.

Davis, A. P., and Capecchi, M. R. (1994). Axial homeosis and appendicular skeleton defects in mice with a targeted disruption of *hoxd-11*. *Development* 120, 2187–2198.

Davis, A. P., Witte, D. P., Hsieh-Li, H. M., Potter, S. S., and Capecchi, M. R. (1995). Absence of radius and ulna in mice lacking *hoxa-11* and *hoxd-11*. *Nature* 375, 791–795.

Davis, A. P., and Capecchi, M. R. (1996). A mutational analysis of the 5′ Hox D genes: Dissection of genetic interactions during limb development in the mouse. *Development* 122, 1175–1185.

Deng, C., Thomas, K. R., and Capecchi, M. R.(1993). Location of crossovers during gene targeting with insertion and replacement vectors. *Mol. Cell. Biol.* 13, 2134–2140.

Dodd, J., Morton, S. B., Karagogeos, K., Yamamoto, M., and Jessell, T. M. (1988). Spatial regulation of axonal glycoprotein expression on subsets of embryonic spinal neurons. *Neuron* 1, 105–116.

Dollé, P., Dierich, A., LeMeur, M., Schimmang, T., Schuhbaur, B., Chambon, P., and Duboule, D. (1993). Disruption of the *Hoxd-13* gene induces localized heterochrony leading to mice with neotenic limbs. *Cell* 75, 431–441.

Duboule, D., and Dollé, P. (1989). The structural and functional organization of the murine *Hox* gene family resembles that of *Drosophila* homeotic genes. *EMBO J.* 8, 1497–1505.

Duboule, D. (1991). Patterning in the vertebral limb. *Curr. Opin. Genet. Dev.* 1, 211–216.

Floß, T., Arnold, H.-H., and Braun, T. (1996). Myf-5^{m1}/Myf-6^{m1} compound heterozygous mouse mutants down-regulate Myf-5 expression and exert rib defects: Evidence for long-range *cis* effects on Myf-5 transcription. *Dev. Biol.* 174, 140–147.

Gaunt, S. J., Krumlauf, R., and Duboule, D. (1989). Mouse homeogenes within a subfamily, *Hox-1.4, -2.6* and *-5.1* display similar anteroposterior domains of expression in the embryo, but show stage- and tissue-dependent differences in their regulation. *Development* 107, 131–141.

Gaunt, S. J., Coletta, P. L., Pravtcheva, D., and Sharpe, P. T. (1990). Mouse Hox-3.4: Homeobox sequence and embryonic expression patterns compared with other members of the Hox gene network. *Development* 109, 329–339.

Geada, A. M., Gaunt, S. J., Azzawi, M., Shimeld, S. M., Pearce, J., and Sharpe, P. T. (1992). Sequence and embryonic expression of the murine *Hox-3.5* gene. *Development* 116, 497–506.

Gendron-Maguire, M., Mallo, M., Zhang, M., and Gridley, T. (1993). *Hoxa-2* mutant mice exhibit homeotic transformation of skeletal elements derived from cranial neural crest. *Cell* 75, 1317–1331.

Gonzales-Reyes, A., and Morata, G. (1990). The developmental effect of overexpressing a *Ubx* product in *Drosophila* embryos is dependent on its interactions with other homeotic products. *Cell* 61, 515–522.

Goto, J., Miyabayashi, T., Wakamatsu, Y., Takahashi, N., and Muramatsu, M. (1993). Organization and expression of mouse *Hox 3* cluster genes. *Mol. Gen. Genet.* 239, 41–48.

Graham, A., Papalopulu, N., and Krumlauf, R. (1989). The murine

and *Drosophila* homeobox gene complexes have common features of organization and expression. *Cell* 57, 367–378.

Hafen, E., Levine, M., and Gehring, W. J. (1984). Regulation of *Antennapedia* transcript distribution by the *bithorax* complex in *Drosophila*. *Nature* 307, 287–289.

Horan, G. S. B., Wu, K., Wolgemuth, D. J., and Behringer, R. R. (1994). Homeotic transformation of cervical vertebrae in *Hoxa-4* mutant mice. *Proc. Natl. Acad. Sci. USA* 91, 12644–12648.

Horan, G. S. B., Kovàcs, E. N., Behringer, R. R., and Featherstone, M. S. (1995a). Mutations in paralogous *Hox* genes result in overlapping homeotic transformations of the axial skeleton: Evidence for unique and redundant function. *Dev. Biol.* 169, 359–372.

Horan, G. S. B., Ramírez-Solis, R., Featherstone, M. S., Wolgemuth, D. J., Bradley, A., and Behringer, R. R. (1995b). Compound mutants for the paralogous *hoxa-4*, *hoxb-4*, and *hoxd-4* genes show more complete homeotic transformations and a dose-dependent increase in the number of vertebrae transformed. *Genes Dev.* 9, 1667–1677.

Hsieh-Li, H. M., Witte, D. P., Weinstein, M., Branford, W., Li, H., Small, K., and Potter, S. S. (1995). *Hoxa 11* structure, extensive antisense transcription and function in male and female fertility. *Development* 121, 1373–1385.

Jeannotte, L., Lemieux, M., Charron, J., Poirier, F., and Robertson, E. J. (1993). Specification of axial identity in the mouse: Role of the *Hoxa-5* (*Hox-1.3*) gene. *Genes Dev.* 7, 2085–2096.

Jegalian, B. G., and DeRobertis, E. M. (1992). Homeotic transformations in the mouse induced by overexpression of a human *hox-3.3* transgene. *Cell* 71, 901–910.

Kessel, M., Balling, R., and Gruss, P. (1990). Variations of cervical vertebrae after expression of a *Hox-1.1* transgene in mice. *Cell* 61, 301–308.

Kessel, M., and Gruss, P. (1991). Homeotic transformations of murine vertebrae and concomitant alteration of *Hox* codes induced by retinoic acid. *Cell* 67, 89–104.

Kostic, D., and Capecchi, M. R. (1994). Targeted disruptions of the murine *hoxa-4* and *hoxa-6* genes result in homeotic transformations of components of the vertebral column. *Mech. Dev.* 46, 231–247.

Kuziora, M. A., and McGinnis, W. (1988). Autoregulation of a Drosophila homeotic selector gene. *Cell* 55, 477–485.

LeMouellic, H., Lallemand, Y., and Brûlet, P. (1992). Homeosis in the mouse induced by a null mutation in the *Hox-3.1* gene. *Cell* 69, 251–264.

Lufkin, T., Dierich, A., LeMeur, M., Mark, M., and Chambon, P. (1991). Disruption of the *Hox-1.6* homeobox gene results in defects in a region corresponding to its rostral domain of expression. *Cell* 66, 1105–1119.

Lufkin, T., Mark, M., Hart, C. P., Dollé, P., LeMeur, M., and Chambon, P. (1992). Homeotic transformation of the occipital bones of the skull by ectopic expression of a homeobox gene. *Nature* 359, 835–841.

Malicki, J., Cianetti, L. C., Peschle, C., and McGinnis, W. (1992). A human *HOX4B* regulatory element provides head specific expression in *Drosophila* embryos. *Nature* 358, 345–347.

Manley, N. R., and Capecchi, M. R. (1995). The role of *hoxa-3* in mouse thymus and thyroid development. *Development* 121, 1989–2003.

Mansour, S. L., Goddard, J. M., and Capecchi, M. R. (1993). Mice homozygous for a targeted disruption of the proto-oncogene *int-2* have developmental defects in the tail and inner ear. *Development* 117, 13–28.

Mark, M., Lufkin, T., Vonesch, J. L., Ruberte, E., Olivo, J.-C., Dollé, P., Gorry, P., Lumsden, A., and Chambon, P. (1993). Two rhombomeres are altered in *Hoxa-1* mutant mice. *Development* 119, 319–338.

McGinnis, N., Kuziora, M. A., and McGinnis, W. (1990). Human *Hox-4.2* and Drosophila *Deformed* encode similar regulatory specificities in Drosophila embryos and larvae. *Cell* 63, 969–976.

McLain, K., Schreiner, C., Yager, K. L., Stock, J. L., and Potter, S. S. (1992). Ectopic expression of *Hox-2.3* induces craniofacial and skeletal malformations in transgenic mice. *Mech. Dev.* 39, 3–16.

McMahon, A., and Bradley, A. (1990). The *Wnt-1* (*int-1*) proto-oncogene is required for development of a large region of the mouse brain. *Cell* 62, 1073–1085.

Patapoutian, A., Yoon, J. K., Miner, J. H., Wang, S., Stark, K., and Wold, B. (1995). Disruption of the mouse MRF4 gene identifies multiple waves of myogenesis in the myotome. *Development* 121, 3347–3358.

Pollock, R. A., Jay, G., and Bieberich, C. J. (1992). Altering the boundaries of Hox 3.1 expression: Evidence for antipodal gene regulation. *Cell* 71, 911–923.

Pollock, R. A., Sreenath, T., Ngo, L., and Bieberich, C. J. (1995). Gain of function mutations for paralogous *Hox* genes: Implications for the evolution of *Hox* gene function. *Dev. Biol.* 92, 4492–4496.

Ramirez-Solis, R., Zheng, H., Whiting, J., Krumlauf, R., and Bradley, A. (1993). *Hoxb-4* (*Hox-2.6*) mutant mice show homeotic transformation of a cervical vertebra and defects in the closure of the sternal rudiments. *Cell* 73, 279–294.

Rancourt, D. E., Tsuzuki, T., and Capecchi, M. R. (1995). Genetic interaction between *hoxb-5* and *hoxb-6* is revealed by nonallelic noncomplementation. *Genes Dev.* 9, 108–122.

Rijli, F. M., Mark, M., Lakkaraju, S., Dierich, A., Dollé, P., and Chambon, P. (1993). A homeotic transformation is generated in the rostral branchial region of the head by disruption of *Hoxa-2*, which acts as a selector gene. *Cell* 75, 1333–1349.

Saegusa, H., Takahashi, N., Noguchi, S., and Suemori, H. (1996). Targeted disruption in the mouse *Hoxc-4* locus results in axial skeleton homeosis and malformation of the xiphoid process. *Dev. Biol.* 174, 55–64.

Samarasinghe, D. D. (1972). Some observations on the innervation of the striated muscle in the mouse oesophagus—An electron microscope study. *J. Anat.* 112, 173–184.

Satokata, I., Benson, G., and Maas, R. (1995). Sexually dimorphic sterility phenotypes in *Hoxa10*-deficient mice. *Nature* 374, 460–463.

Simeone, A., Pannese, M., Acampora, D., D'Esposito, M., and Boncinelli, E. (1988). At least three human homeoboxes on chromosome 12 belong to the same transcription unit. *Nucleic Acids Res.* 16, 5379–5389.

Small, K. M., and Potter, S. S. (1993). Homeotic transformations and limb defects in *Hoxa-11* mutant mice. *Genes Dev.* 7, 2318–2328.

Struhl, G., and White, R. A. H. (1985). Regulation of the *Ultrabithorax* gene of Drosophila by other Bithorax complex genes. *Cell* 43, 507–519.

Suemori, W., Takahashi, N., and Noguchi, S. (1995). *Hoxc-9* mutant mice show anterior transformation of the vertebrae and malformation of the sternum and ribs. *Mech. Dev.* 51, 265–273.

Thomas, K. R., and Capecchi, M. R. (1987). Site-directed mutagene-

sis by gene targeting in mouse embryo-derived stem cells. *Cell* 51, 503–512.

Wall, N. A., Jones, C. M., Hogan, B. L. M., and Wright, C. V. E. (1992). Expression and modification of *hox-2.1* protein in mouse embryos. *Mech. Dev.* 37, 111–120.

Wolgemuth, D. J., Behringer, R. R., Mostoller, M. P., Brinster, R. L., and Palmiter, R. D. (1989). Transgenic mice overexpressing the mouse homeobox-containing gene *Hox-1.4* exhibit abnormal gut development. *Nature* 337, 464–467.

Zhang, W., Behringer, R. R., and Olson, E. N. (1995). Inactivation of the myogenic bHLH gene *MRF4* results in up-regulation of myogenin and rib anomalies. *Genes Dev.* 9, 1388–1399.

Received for publication February 16, 1996
Accepted April 15, 1996